Polarimetric Properties of Chaff

DUŠAN S. ZRNIĆ

National Severe Storms Laboratory, Norman, Oklahoma

ALEXANDER V. RYZHKOV

Cooperative Institute for Mesoscale Meteorological Studies, University of Oklahoma, Norman, Oklahoma

(Manuscript received 28 October 2003, in final form 30 January 2004)

ABSTRACT

Chaff contaminates estimates of precipitation amounts; hence, it is important to remove (or censor) its presence from the fields of radar reflectivity. It is demonstrated that efficient and direct identification of chaff is possible with a polarimetric radar. Specifically considered are the horizontal and vertical polarization basis and covariances of corresponding returned signals. Pertinent polarimetric variables are the copolar correlation coefficient, differential reflectivity, and the linear depolarization ratio. Two models are used to compute the expected values of these variables. In one, chaff is approximated with a Hertzian dipole and, in the other, with a thin wire antenna. In these models chaff is assumed to have a uniform distribution of flutter angles (angle between the horizontal plane and chaff axis). The two models produce nearly equivalent results. Also shown are polarimetric signatures of chaff observed in the presence of precipitation. Inferences about chaff's orientation are made from comparisons between measured and observed differential reflectivity and the cross-correlation coefficient.

1. Introduction

Chaff is made of aluminum-coated thin fibers and is released by the military to create widespread echoes and, thus, confuse noncooperating tracking radars. To maximize backscattering cross section, chaff length is chosen to equal one-half radar wavelength. As predominant wavelengths for military surveillance and tracking are 3, 5, and 10 cm, the standard chaff lengths are 1.5, 2.5, and 5 cm. Because chaff is employed by the military as part of routine training in the United States, it is often observed as echoes on weather radars (Maddox et al. 1997). Although the reflectivity is relatively weak, it is sufficient to contaminate precipitation estimates (Vasiloff and Struthwolf 1997). Examples abound in the western United States whereby chaff is embedded in precipitation (opus cited) or coexist next to precipitation echoes (Ziegler et al. 2001; Brandt and Atkin 1998). Thus, it is desirable to recognize returns due to chaff and censor these from precipitation products.

It has been argued (Zrnić and Ryzhkov 1999) that polarimetric radar offers a simple and effective way to identify chaff. The argument is rooted in common sense logic and experimental evidence gained with circularly polarized radars (Brooks et al. 1992). Polarimietric signatures of chaff in a linear horizontal and vertical basis have not been reported. Moreover, because chaff is a nuisance (as far as observation of weather is concerned), little or no theoretical results about its polarimertric properties are available. In a few years the National Weather Service will add polarimetric capability to its network of WSR-88Ds. Therefore, it will soon be possible to have a simple automated procedure for censoring chaff. Our purpose herein is to present scattering models of chaff that capture the essential polarimetric properties as well as some data to support these properties.

In laminar airflow, chaff is mostly horizontally oriented and slowly falls with respect to air. Turbulence and differential air motion will cause wobbling. In either case differential reflectivity Z_{DR} is expected to be relatively large. The linear depolarization ratio L_{DR} will increase compared to the value in precipitation and the cross-correlation between copolar returns ρ_{hv} will decrease. These polarimetric variables do not depend on the absolute values of returned power (i.e., backscattering cross section), yet they are the most significant discriminators. It is the insensitivity to the cross section that simplifies model development.

Two simple models for computing polarimetric properties of chaff come to mind. In one the chaff is approximated with the Hertzian dipole so that standard formulas (i.e., for prolate spheroids with induced field along the axis and no field perpendicular) could be ap-

Corresponding author address: Dr. Dušan S. Zrnić, National Severe Storms Laboratory, Doppler Radar and Remote Sensing Research, 1313 Halley Circle, Norman, OK 73069.
E-mail: dusan.zrnic@noaa.gov

plied to compute the elements of the covariance matrix. This approximation is applicable for chaff lengths much shorter than the wavelength. But, for polarimetric variables independent of concentration and backscattering cross section we show that the model can be extended to half-wavelength sizes.

A more realistic approach is to model chaff as a thin cylindrical antenna and apply standard formulas to obtain the scattering coefficients. This second approach is also explored herein. Then, once the scattering coefficients are determined, the geometrical transformations, as done for spheroids (Bringi and Chandrasekhar 2001; Ryzhkov 2001), can be used for computation of the polarimetric variables.

The underlying assumption in our models is that chaff does not clump and does not flex on the way to the ground. To compute the fields of flexing and/or clumping chaff two steps are needed. First, a physical model is required to describe the flexing and/or clumping geometry. Then a numerical solution, such as a discrete dipole approximation (Evans and Vivekanandan 1990), should be applied to this geometry to obtain the scatter coefficients. Because the extent of clumping and/or flexing is not known, we consider only rigid chaff without clumps for which the thin antenna model is very well suited.

Both of our models can be applied to determine chaff concentration N_o within the resolution volume from a relation between volume reflectivity η ($m^2\ m^{-3}$) and specific differential phase K_{DP}. This is significant for studies of diffusion in the atmosphere (e.g., Hildebrand 1977). Whereas this and similar studies (Martner et al. 1992) relied on sample volume-weighted averages over the chaff field, the polarimetric method allows much finer resolution. It is possible to achieve about 1-km resolution in the radial direction (sufficient for estimating specific differential phase) and the intrinsic beamwidth dictates the transverse resolution.

2. Models

a. Hertzian dipole

Patterned after a prolate spheroid, this model in general can be thought of as composed of two orthogonal dipoles: One has fixed orientation along the chaff axis, the other is induced perpendicular to the axis. The dipole along the chaff axis is dominant and will be used initially to compare this simple model with a thin wire model. This model is strictly valid for chaff lengths much smaller than the wavelength. Nonetheless, it turns out that its results compare fairly well to the thin wire model. Let the scattering amplitude for the E field along the axis be f_a and the amplitude for the perpendicular field be f_b. For a perfect conductor the two amplitudes will be in phase. Therefore, without loss of substance we assume these to be real. Then, as shown by Holt and Shepherd (1979), we write the backscattering matrix $\mathbf{S}$

$$\mathbf{S} = \begin{bmatrix} (f_a - f_b)\sin^2(\psi)\sin^2(\alpha) + f_b & (f_a - f_b)\sin^2(\psi)\sin(\alpha)\cos(\alpha) \\ (f_a - f_b)\sin^2(\psi)\sin(\alpha)\cos(\alpha) & (f_a - f_b)\sin^2(\psi)\cos^2(\alpha) + f_b \end{bmatrix}. \quad (1)$$

In (1) ψ is the angle between the axis of chaff and the propagation vector and α is the canting angle; the equation is valid for Rayleigh scatterers (i.e., small compared to wavelength).

Next we list equations for the components of the covariance scattering matrix, which determine the polarimetric variables studied herein. The assumption is that multiple scattering is insignificant, all chaff needles have same size, and there is a distribution of orientation. Following Ryzhkov (2001), the pertinent elements are

$$\begin{aligned} \langle|s_{hh}|^2\rangle &= \langle|f_b|^2\rangle - 2\langle(f_b^2 - f_a f_b)A_2\rangle + \langle|f_b - f_a|^2 A_4\rangle, \\ \langle|s_{vv}|^2\rangle &= \langle|f_b|^2\rangle - 2\langle(f_b^2 - f_a f_b)A_1\rangle + \langle|f_b - f_a|^2 A_3\rangle, \\ \langle|s_{hv}|^2\rangle &= \langle|s_{vh}|^2\rangle = \langle|f_b - f_a|^2 A_5\rangle, \quad \text{and} \\ \langle s_{hh}^* s_{vv}\rangle &= \langle|f_b|^2\rangle + \langle|f_b - f_a|^2 A_5\rangle - \langle(f_b - f_a f_b)A_1\rangle \\ &\quad - \langle(f_b^2 - f_a f_b)A_2\rangle. \end{aligned} \quad (2)$$

In these equations the A_i are products of sinusoidal functions

$$\begin{aligned} A_1 &= \sin^2(\psi)\cos^2(\alpha), \\ A_2 &= \sin^2(\psi)\sin^2(\alpha), \\ A_3 &= \sin^4(\psi)\cos^4(\alpha), \\ A_4 &= \sin^4(\psi)\sin^4(\alpha), \\ A_5 &= \sin^4(\psi)\cos^2(\alpha)\sin^2(\alpha). \end{aligned} \quad (3)$$

Assume that the chaff is randomly oriented in the horizontal plane (i.e., azimuth angle φ is between 0 and 2π), the radar elevation is 0° (a good approximation for surveillance radars), and the angle between axis of chaff and horizontal plane is uniformly distributed from 0 to $\pi/2 - \theta_1$ (angle θ_1 is measured with respect to the true vertical). Henceforth, the maximum deviation ($\pi/2 - \theta_1$) will be referred to as ''flutter angle.'' Thus, a probability density function that represents a uniform distribution of orientation within the above prescribed limits is given by

$$p(\theta, \varphi) = \sin(\theta)/[2\pi\cos(\theta_1)]. \quad (4)$$

The relations between the α, ψ and θ, φ angles

$$\sin(\theta)\cos(\varphi) = \sin(\alpha)\sin(\psi),$$
$$\cos(\theta) = \sin(\psi)\cos(\alpha), \quad \text{and}$$
$$\cos(\psi) = \sin(\theta)\sin(\varphi), \tag{5}$$

are needed to integrate various terms in Eq. (2). Two of the equations in (5) are independent, but three are listed for convenience (these are substituted into various integrands).

Next the scattering amplitudes are assumed fixed and the transverse amplitude $f_b = 0$. Then integration with the prescribed distribution produces the following closed form solutions for the angular moments $\langle A_i \rangle$:

$$\langle A_1 \rangle = \cos^2(\theta_1)/3,$$
$$\langle A_2 \rangle = [\sin^2(\theta_1)/6 + 1/3],$$
$$\langle A_3 \rangle = \cos^4(\theta_1)/5,$$
$$\langle A_4 \rangle = 3[\sin^4(\theta_1) - 4\cos^2(\theta_1)/3 + 4]/40,$$
$$\langle A_5 \rangle = [\cos^2(\theta_1)/3 - \cos^4(\theta_1)/5]/2. \tag{6}$$

These will be used shortly to plot the polarimetric variables Z_{DR}, ρ_{hv}, L_{DR}, and the ratio $(K_{DP})^2/\eta$. The cross to copolar correlations ρ_{xh} and ρ_{xv} are zero for chaff with a random horizontal orientation and zero mean flutter angle.

b. Thin cylindrical antenna

In this model chaff is represented as a thin cylindrical antenna of length L and radius a. The antenna is illuminated by a plane wave, the angle between the antenna axis and the propagation direction is ψ; and the electric field, the antenna, and the propagation vector are in a common plane. It is accepted practice to assume the following sinusoidal distribution of the induced current along the antenna:

$$I(l) = I_m \sin\left[\frac{2\pi}{\lambda}\left(\frac{L}{2} - |l|\right)\right], \tag{7}$$

where I_m is the maximum value of the current (depending on ψ), the wavenumber $k = 2\pi/\lambda$, and l is distance to the antenna midpoint. Further, the midpoint also serves as the phase reference.

The antenna impedance Z_i, the incident electric field along the antenna $E_l = E\sin(\psi)\exp[-jkl\cos(\psi)]$, the current $I(0)$, and the distribution (7) satisfy [Jordan and Balmain 1968, Eqs. (14)–(16)]

$$Z_i = -\frac{1}{I^2(0)}\int_{-L/2}^{L/2} E_l I(l)\, dl. \tag{8}$$

Obviously, the plane wave electric field at the antenna location has a magnitude E; harmonic time dependence is assumed (but not explicitly written) for all fields and currents.

Substitution of (7) into (8) relates I_m, Z_i, and E. Further, values of Z_i can be computed from a relatively cumbersome formula if the thickness, length, and wavelength of the thin antenna are known (Krauss 1950). The current distribution induced by the incident field produces a field at a range r (far from the antenna) given by Eq. (5-81) in Krauss (1950). After elimination of I_m the final expression for this electric field is

$$E_\psi = -j\frac{60E\lambda}{rZ_i\pi\sin^2(\pi L/\lambda)} \times \left\{\frac{\cos[kL\cos(\psi)/2] - \cos(kL/2)}{\sin(\psi)}\right\}^2. \tag{9}$$

There are no other field components [the units in (9) are MKS and ''60'' has the unit ohms, which comes from the characteristic impedance of free space]. Therefore, the scattering coefficient s_{yy} can be obtained by omitting $-j$, r, and E from Eq. (9):

$$s_{yy} = \frac{60\lambda}{Z_i\pi(\sin^2(\pi L/\lambda)}\left\{\frac{\cos[kL\cos(\psi)/2] - \cos(kL/2)}{\sin(\psi)}\right\}^2. \tag{10}$$

Note that the scattering coefficient s_{yy} is the same for the forward and back direction (because the antenna is axially symmetric). It represents the radiation pattern (amplitude) of the scatterer. The induced electric field perpendicular to the axis will be neglected. Thus, the formalism developed for dipole model (prolate spheroid) can be directly applied to compute elements of the covariance matrix. It suffice to substitute $|s_{yy}|^2$ in place of $f_a^2\sin^2(\psi)$ so that

$$\langle|s_{hh}|^2\rangle = \langle\sin^4(\alpha)|s_{yy}|^2\rangle,$$
$$\langle|s_{vv}|^2\rangle = \langle\cos^4(\alpha)|s_{yy}|^2\rangle,$$
$$\langle|s_{hv}|^2\rangle = \langle|s_{vh}|^2\rangle = \langle\sin^2(\alpha)\cos^2(\alpha)|s_{yy}|^2\rangle,$$
$$\langle s_{hh}^* s_{vv}\rangle = \langle\sin^2(\alpha)\cos^2(\alpha)|s_{yy}|^2\rangle. \tag{11}$$

Integrals in (11) are two-dimensional (over θ, φ) and no closed form solutions are possible (except in some trivial cases, like for $\theta_1 = \pi/2$). Hence one resorts to numerical integration.

c. Results of computations

Next, three polarimetric variables are computed for the two models previously described. These are

differential reflectivity:

$$Z_{DR} = 10\log(\langle|s_{hh}|^2\rangle/\langle|s_{vv}|^2\rangle),$$

copolar cross-correlation coefficient:

$$\rho_{hv} = \langle s_{hh}^* s_{vv}\rangle/(\langle|s_{hh}|^2\rangle\langle|s_{vv}|^2\rangle)^{1/2},$$

linear depolarization ratio:

$$L_{DR} = 10\log(\langle|s_{vh}|^2\rangle/\langle|s_{hh}|^2\rangle). \tag{12}$$

Under the assumption that the induced field transverse

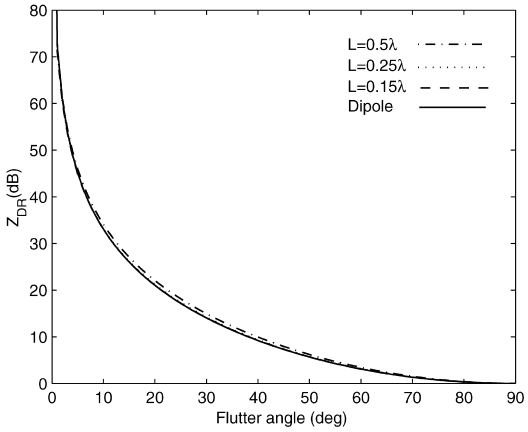

FIG. 1. Differential reflectivity as a function of the flutter angle, defined as the maximum (positive as well as negative) deviation of the chaff axis from the horizontal plane. The lengths of modeled chaff as a thin antenna model are indicated in terms of wavelength.

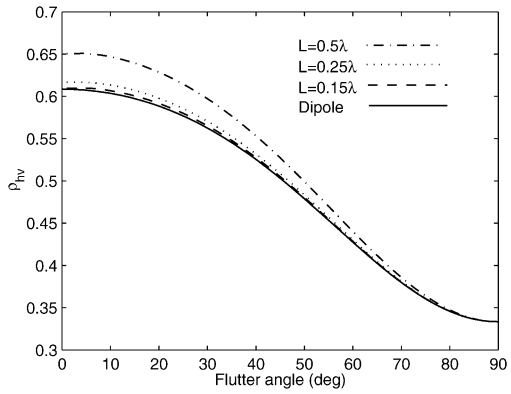

FIG. 2. Cross-correlation coefficient for the same models as in Fig. 1.

to the chaff axis is negligible [as written in Eq. (11)], these three variables are related via

$$L_{DR} = \rho_{hv}(Z_{DR})^{-1/2}, \tag{13}$$

wherein L_{DR} and Z_{DR} are expressed in linear units.

The three variables (12) are plotted in Fig. 1, 2, and 3 for both models. The fluttering angle in these figures is between the chaff axis and the horizontal plane (equal to $\pi/2 - \theta_1$). Also, three lengths of chaff are used in the antenna model. The choice is such that for a 10-cm wavelength radar, chaff needles are 5, 2.5, and 1.5 cm; these are standard chaffs for confusing radars with wavelengths of 10, 5, and 3 cm, respectively. A glaring conclusion is that the difference in Z_{DR} and L_{DR} for the two models is insignificant. The difference in the ρ_{hv} (at small flutter − wobbling) is inconsequential for the purpose of identifying chaff.

Further, practical radars are limited in measurements of these polarimetric variables. For example, the minimum L_{DR} due to coupling through the system is about −30 dB, which means that only wobbling by more than about ±4° could be discerned (Fig. 3). A more stringent limit to both estimates of L_{DR} and Z_{DR} is the receiver noise power that would overwhelm the weaker signal. Bias in these estimates due to receiver noise can be eliminated, but the variance at low signal-to-noise ratios (SNRs) increases.

Comparison of the three variables from the two models suggests that the simple dipole is quite adequate to explain the dependence on the wobbling (fluttering) angle. This dependence is mostly due to the orientation of the chaff needles (or dipole moments) and is little affected by the angular dependence of the scattering coefficients. This independence is expected for chaff lengths that produce one lobe of the backscatter pattern. Although this lobe is sharper for the thin antenna than the dipole, it makes little difference to the variables on average.

The rather large values in Z_{DR} predicted for flutter angles between 0° and 40° require some explanation. Without direct measurement we speculate that four factors at play might prevent such large values: 1) it could be that natural wobbling is larger, 2) induced field transverse to the chaff axis might be present, 3) there could be some flexing of the chaff as it falls, and 4) the weaker signal (in the vertical channel) is below noise level.

The antenna model does have an advantage if one is interested in the backscattering cross section or specific differential phase. It can predict fairly well the magnitudes of the scattering coefficients provided that the size of chaff is known. With this knowledge one could possibly determine the number density of chaff from the reflectivity factor and/or specific differential phase. But there are no compelling reasons to estimate chaff density unless it could be used to separate its contribution from precipitation in the same resolution volume. At the moment this is a remote possibility, whereas

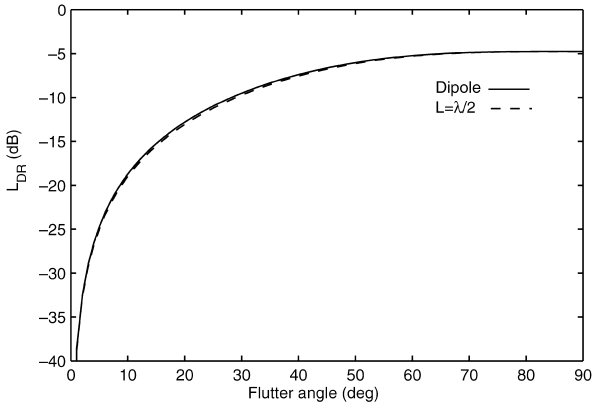

FIG. 3. Linear depolarization ratios for a dipole and thin resonant chaff. Results for other smaller lengths are indistinguishable from the dipole model.

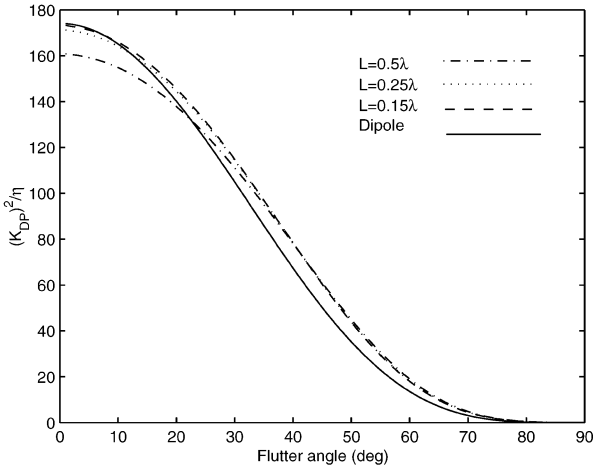

FIG. 4. Ratio $(K_{DP})^2/\eta$ for the thin wire model (lengths as fractions of wavelength are indicated) and the dipole model. The ordinate is in units of $\lambda^2 N_o$.

censoring chaff is waiting to be applied on the future polarimetric WSR-88D.

3. Chaff density

Next we present a formalism for computing chaff density. This can be achieved by measuring the specific differential phase K_{DP} and volume reflectivity.

By definition, for the Hertzian dipole model of chaff

$$K_{DP} = 180\lambda f_a N_o(\langle A_2\rangle - \langle A_1\rangle)/\pi = 180\lambda f_a N_o \sin^2(\theta_1)/(2\pi) \quad (^\circ\ \mathrm{m}^{-1}), \qquad (14)$$

where the units for λ and f_a are meters and concentration N_o is per cubic meter. Further, it is assumed that the imaginary part of f_a is zero.

In the case of a thin antenna the equation becomes

$$K_{DP} = 180\lambda N_o[\langle \sin^2(\alpha)|s_{yy}|\rangle - \langle \cos^2(\alpha)|s_{yy}|\rangle]/\pi. \qquad (15)$$

The volume reflectivity η (at horizontal polarization) is related to the scattering coefficients by

$$\eta = 4\pi N_o\langle |s_{hh}|^2\rangle. \qquad (16)$$

For the Hertzian dipole substitute $\langle |s_{hh}|^2\rangle = |f_a|^2\langle A_4\rangle$ in (16), square (14), and divide with (16) to obtain

$$\frac{(K_{DP})^2}{\eta} = \frac{2025\ \sin^4(\theta_1)}{\pi^3[\sin^4(\theta_1) - 4\ \cos^2(\theta_1)/3 + 4]}\lambda^2 N_o. \qquad (17)$$

Clearly this ratio depends on the radar wavelength, flutter angle $(\pi 2 - \theta_1)$, and concentration. Computations for the thin antenna model require similar substitution but with $\langle |s_{hh}|^2\rangle$ from (11) into (16), then squaring (15), and dividing with (16). Note units in (17) are in MKS, and K_{DP} is in degrees per meter. It happens that the result is the same if units of K_{DP} are changed to the more representative degrees per kilometer and η is in millimeters squared per cubic meter.

Plots of (17) and similar values for the thin antenna (Fig. 4) indicate that the multiplying factor (in units of $\lambda^2 N_o$) is relatively insensitive to the chaff length. Further, it changes by less than 20% for small flutter angles ($<20^\circ$). Thus, in such instances it might be possible to determine chaff concentration if the return at vertical polarization is sufficiently strong for accurate estimation of K_{DP}. Similar reasoning might be applied to determine concentration of monodispersed ice needles.

4. Experimental data

On 6 February 2003, a cloud of ice crystals (henceforth, snowband) was observed initially over northwest Oklahoma, following a snowfall event. This feature advected southeastward toward Oklahoma City (Fig. 5). At the same time, a chaff ''cloud'' released from an air force base in eastern New Mexico moved across southern Oklahoma.

The reflectivity structures of the snowband and chaff look very similar, but the polarimetric variables exhibit significant differences. Differential reflectivity of chaff ranges from 0 to 6 dB, whereas for snow it is 0 to 3 dB; hence, there is an overlap of values. The fields of the correlation coefficient uniquely identify chaff and separate fairly well snow from ground clutter except in regions where the SNR in snow is low (at far distances from the radar, see Fig. 5). Total differential phases of chaff and snow (Φ_{DP}) also differ substantially. The differential phase in a region of snow is close to the ''system'' differential phase (of about 30°) and exhibits very small spatial fluctuations. In contrast, the differential phase of chaff is characterized by significant spatial variations.

More detailed analysis of the histogram of Φ_{DP}, prior to radial averaging, in chaff reveals a broad maximum at about 80°. This mean value of Φ_{DP} might be indicative of the ''receiver component'' of the system differential phase. Indeed, physical considerations indicate that chaff produces zero backscatter differential phase. That is, regardless of the transmitted differential phase between the H and V components each needle reflects a field aligned along its axis. Thus, upon reflection the H and V fields are in phase. Once these fields are transformed into voltages and subsequently passed through the receiver, they acquire the differential phase of the receiver. This reasoning is valid if the H and V fields are transmitted simultaneously, as is done in the current implementation on the KOUN radar. In the case of sequential transmission (of H and V components) the backscatter differential phase obtained from chaff is equal to the sum of the transmitted differential phase and differential phase of the receiver (i.e., total differential phase of the radar system). We speculate that very broad distribution of the differential phase in chaff is primarily due to high measurement errors attributed to a very low cross-correlation coefficient (between 0.2 and 0.5). Similar analysis of differential phase in ground

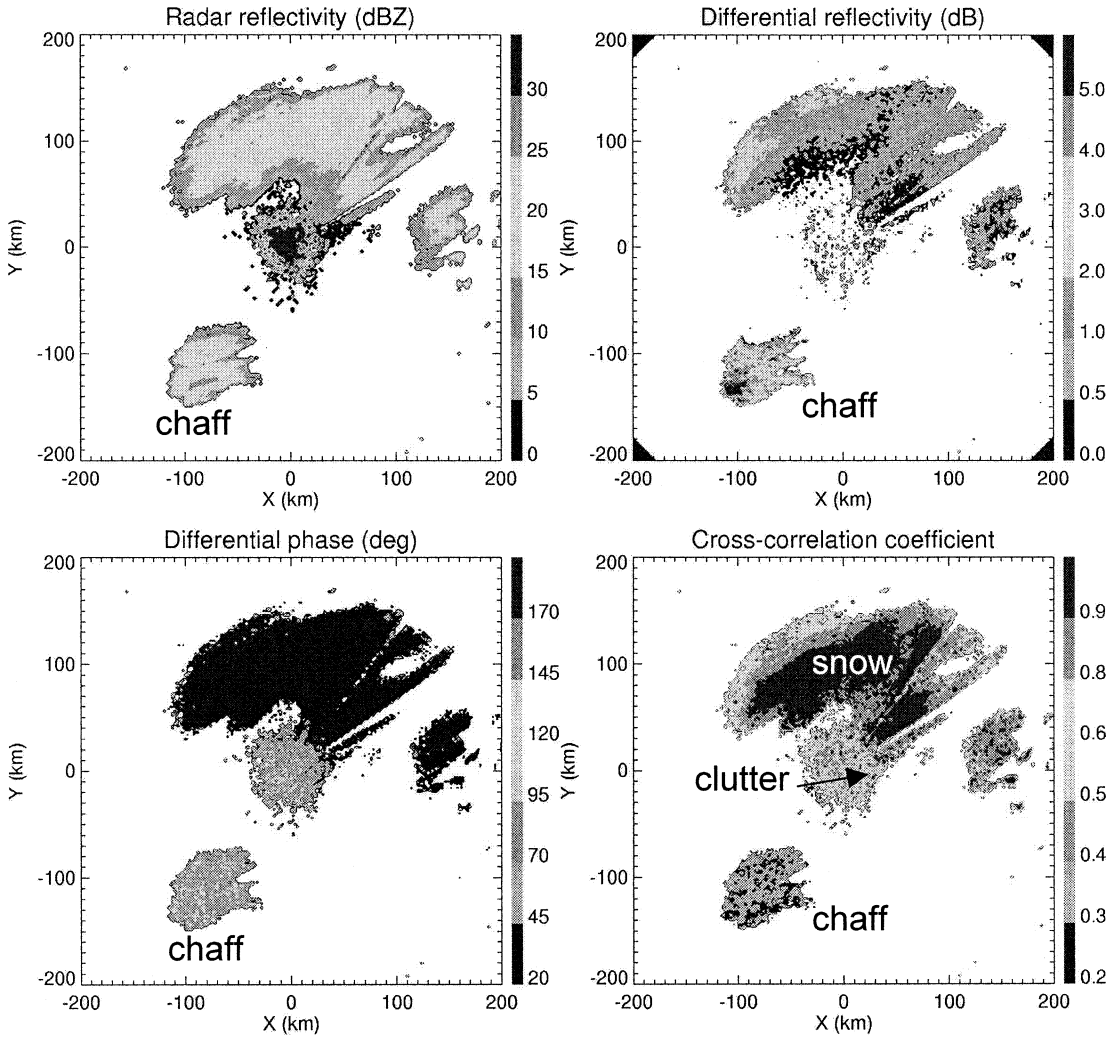

FIG. 5. Fields of polarimetric variables from regions of ground clutter, chaff, and snow. Data were obtained during the Joint Polarization Experiment (JPOLE) at 2100 6 Feb 2003 from a scan at 0.5° elevation.

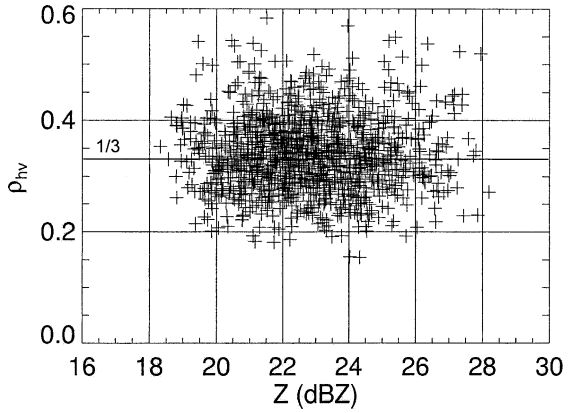

FIG. 6. Scattergram of the correlation coefficient vs reflectivity factor from chaff. Data were collected on 6 Feb 2003.

clutter reveals almost uniform distribution of Φ_{DP} within the interval between 0° and 180°. The ρ_{hv} values from ground clutter are significantly higher than the corresponding values from chaff (Fig. 5); thus one expects smaller measurement errors of Φ_{DP} in ground clutter. The observed uniform distribution of the differential phase from ground clutter indicates that its intrinsic Φ_{DP} (i.e., backscatter differential phase void of any measurement errors) might be uniformly distributed as opposed to chaff for which intrinsic differential phase upon scattering is likely zero.

Scattergrams of differential reflectivity and correlation coefficient versus reflectivity factor at SNRs >10 dB and from the region of chaff are displayed in Figs. 6 and 7. These data are from six scans at 0.5° elevation between 2000 and 2100 UTC. The average value of Z_{DR} is 3.36 dB without noise correction and 2.3 dB with correction; the average of ρ_{hv} is 0.34 without noise correction and 0.36 with correction. For the noise corrected

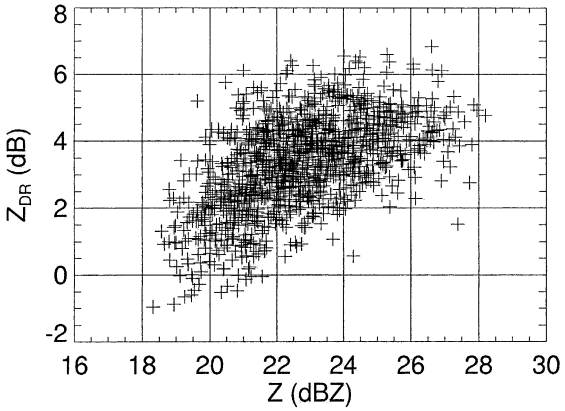

FIG. 7. Scattergram of differential reflectivity vs reflectivity from chaff.

values the model (Figs. 1 and 2) suggests that the flutter angle is 65° (implied from Z_{DR}) and 75° (implied from ρ_{hv}). The agreement is reasonable considering that the model of uniform flutter angle distribution is a crude approximation of the true (but unknown) distribution and that clumping and flexing of chaff could be present. Still, both polarimetric variables indicate that the needles have a large effective variation of flutter angles.

5. Conclusions

Two scattering models have been used to compute polarimetric variables of chaff. The models are a Hertzian dipole and thin wire antenna. Pertinent polarimetric variables are differential reflectivity, correlation coefficient between copolar signals, and linear depolarization ratio. Chaff is assumed to be uniformly distributed in azimuth. The angle between its axis and horizontal plane (flutter angle) is also uniformly distributed but between zero and a maximum value. It follows that the two models produce very similar results if the chaff length is half the radar wavelength or less. The linear depolarization ratio is uniquely related to ρ_{hv} and Z_{DR}; therefore, these two variables are sufficient to separate chaff from precipitation echoes. Nonetheless, chaff could be confused with echoes from insects, which produce similar values of ρ_{hv} and insect Z_{DR} overlaps with the Z_{DR} of birds.

Chaff concentration can be computed from specific differential phase K_{DP} and volume reflectivity η. The values are almost insensitive to the flutter angle; hence it should be possible to estimate concentrations with less than 20% error. Thus, chaff observation with a polarimetric radar offers attractive means for studying diffusion in the atmosphere.

One fortuitous observation of chaff demonstrated significant separation of chaff from ground clutter and snow echoes. There is no overlap of the low-correlation values (0.2–0.5) from chaff with those from ground clutter (0.6–0.8) or snow (0.6–1). Low values from snow (<0.9) are at low signal-to-noise ratios, which occur at distant ranges. Differential reflectivity of chaff is well separated from the one in snow, but in the absence of ρ_{hv} it can be mistaken to originate from rain.

Acknowledgments. We are grateful to R. J. Doviak for help concerning the antenna model and Chris Curtis for suggesting compact ways to numerically integrate two-dimensional integrals. Data presented here were collected during the Joint Polarization Experiment (JPOLE), which was organized by Terry Schuur and partly supported by the Office of System Technology of the National Weather Service. The NWS Radar Operations Center (ROC) contributed the basic RVP7 processor and display, which was subsequently enhanced to process dual-polarization signals. John Carter and Valery Melnikov were responsible for the polarimeric aspects of the radar. Alan Siggia, from Sigmet, resolved numerous technical details needed to operate the RVP7 processor in dual-polarization mode. Mike Schmidt and Richard Wahkinney made extensive modifications of microware circuitry and controls. Allen Zahrai led the team of engineers who designed the new system, which enabled scanning strategies and allowed flexibility. Funding by the NWS Office of Science and Technology and the FAA over the last few years made this research possible.

REFERENCES

Brandt, M. B., and D. V. Atkin, 1998: Chaff in the vicinity of thunderstorms in Southern California on 6 June 1997. NWS Western Region Tech. Attachment No. 98-04. [Available online at http://www.wrh.noaa.gov/wrhq/98TAs/9804/index.html.]

Bringi, V. N., and V. Chandrasekar, 2001: *Polarimetric Doppler Weather Radar, Principles and Applications.* Cambridge University Press, 636 pp.

Brookes, E. M., J. D. Marwitz, and R. A. Kropfli, 1992: Radar observations of transport and diffusion in clouds and precipitation using TRACIR. *J. Atmos. Oceanic Technol.,* **9,** 226–241.

Doviak, R. J., and D. S. Zrnić, 1993: *Doppler Radar and Weather Observations.* 2d ed. Academic Press, 562 pp.

Evans, K. F., and J. Vivekanandan, 1990: Multiparameter radar and microwave radiative transfer modeling of nonspherical atmospheric ice particles. *IEEE Trans. Geosci. Remote Sens.,* **28,** 423–437.

Hildebrand, P. H., 1977: A radar study of diffusion in the lower atmosphere. *J. Appl. Meteor.,* **16,** 493–510.

Holt, A. R., and J. W. Shepherd, 1979: Electromagnetic scattering by dielectric spheroids in the forward and backward directions. *J. Phys. A Math. Gen.,* **12,** 159–166.

Jordan, E. C., and K. G. Balmain, 1968: *Electromagnetic Waves and Radiating Systems.* Prentice-Hall, 753 pp.

Kraus, J. D., 1950: *Antennas.* McGraw-Hill 553 pp.

Maddox, R. A., K. W. Howard, and C. L. Dempsey, 1997: Intense convective storms with little or no lightning over central Arizona: A case of inadvertent weather modification? *J. Appl. Meteor.,* **36,** 302–314.

Martner, B. E., J. D. Marwitz, and R. A. Kropfli, 1992: Radar observations of transport and diffusion in clouds and precipitation using TRACIR. *J. Atmos. Oceanic Technol.,* **9,** 226–242.

Ryzhkov, A. V., 2001: Interpretation of polarimetric radar covariance matrix for meteorological scatterers: Theoretical analysis. *J. Atmos. Oceanic Technol.,* **18,** 315–328.

Vasiloff, S., and M. Struthwolf, 1997: Chaff mixed with radar weather echoes. NWS Western Region Tech. Attachment No. 97-02, 8 pp. [Available online at http://www.wrh.noaa.gov/wrhq/97TAs/TA9702/ta97-02.html.]

Ziegler, C. L., E. N. Rasmussen, T. R. Shepherd, A. I. Watson, and J. M. Straka, 2001: Evolution of low-level rotation in the 29 May 1994 Newcastle–Graham, Texas, storm complex during VORTEX. *Mon. Wea. Rev.*, **129,** 1339–1368.

Zrnić, D. S., and A. Ryzhkov, 1999: Polarimetry for weather surveillance radar. *Bull. Amer. Meteor. Soc.*, **80,** 389–406.